Phenol−(Ethanol)$_1$ Isomers Studied by Double-Resonance Spectroscopy and ab Initio Calculations

D. Spangenberg, P. Imhof, W. Roth,[†] Ch. Janzen, and K. Kleinermanns*

Institut für Physikalische Chemie und Elektrochemie I, Heinrich Heine Universität Düsseldorf, Universitätsstrasse 1, 40225 Düsseldorf, Germany

Received: March 3, 1999; In Final Form: May 24, 1999

The jet-cooled 1:1 complex of phenol and ethanol was studied by several laser spectroscopic techniques and ab initio calculations at the Hartree−Fock 6-31G(d,p) level. The laser-induced fluorescence (LIF) and mass-selected resonant two-photon ionization (R2PI) spectra showed that the electronic $S_1 \leftarrow S_0$ origin consists of two transitions separated by 2 cm^{-1}. The dispersed fluorescence (DF) and IR−UV and UV−IR double-resonance spectra reveal that these transitions are the electronic origins of two different isomers. The ab initio calculations yield three minimum energy structures of anti/gauche conformers of the ethanol moiety in the hydrogen-bonded cluster. The comparison of the experimental and theoretical results allows an assignment of the spectral features to the calculated rotamer structures.

1. Introduction

The investigation of small- and medium-sized clusters is of long-standing interest with the clusters as microscopic model systems for an understanding of macroscopic solvation phenomena. Hydrogen-bonded systems are of particular relevance in physics, chemistry, and biology. The complexes of an aromatic chromophore like phenol allow a cluster size and isomer-specific investigation by using double-resonance spectroscopy based on ionization techniques and dispersed fluorescence of selected vibronic levels. The shift of the electronic spectra depends on the proton donor or acceptor interaction of the phenolic OH group with the solvent,[1] a “molecular solvatochromism”. IR spectra of these clusters in molecular beams reveal structural differences in the hydrogen-bonded network.[9,34] Specific information about the cluster structures and strengths of interaction can be derived from the electronic and vibrational shifts. Surely, a predominant effect results from the nature of the solvent itself. This was shown by the work done on clusters of phenol with various hydrogen-bonding molecules such as ammonia,[2,3] amines,[4] ethers, alcohols,[5,6,36] and water (e.g., ref 7 and references therein) and very recently also on carboxylic acids.[8]

Different orientations of molecules within the hydrogen-bonded network show a much weaker effect. Experimentally, it was possible to identify two isomers of D_{2d} and S_4 symmetries of the $(H_2O)_8$ moiety in benzene−$(H_2O)_8$,[9] the corresponding isomers of bare $(H_2O)_8$,[10] two analogous phenol−$(H_2O)_7$ structures, and three phenol−$(H_2O)_8$ isomers.[11]

The characterization of different rotamers in a hydrogen-bonded system is an even more demanding challenge. Ethanol (EtOH) is one of the most simple examples of a hydrogen-bonding solvent that consists of nonequivalent conformers. These are one anti and two enantiomeric gauche rotamers. They convert into each other by a rotation of the OH group relative to the CH frame. The existence of two conformers in the gas phase was already demonstrated in 1936 by overtone spectroscopy of the OH stretching vibration.[12] Later on, measurements of bare ethanol in the gas phase,[13−17] in nonpolar solvents,[13,18,19] and in matrixes[20,21] showed that the anti species should be the most stable conformer and that its OH stretching vibration is about 5−15 cm^{-1} blue-shifted relative to that of the gauche isomer (3676 versus 3660 cm^{-1} in the gas phase). This blue shift was explained by Krueger et al. as result of a trans lone pair effect.[22] Analysis of microwave rotational spectra gave a gauche/anti energy difference of 41.2 ± 0.5 cm^{-1},[23] while the temperature dependence of the OH overtone spectra gave a free enthalpy difference of 245 ± 35 cm^{-1}.[16]

Several theoretical attempts gave contradictory results of the stability sequence.[24,25] Bakke and Bjerkeseth showed in a large survey that either semiempirical or ab initio methods gave consistently the same frequency order of both OH stretching vibrations[26] (see above).

Up to now, there has been only a small number of publications concerning the phenol−EtOH cluster. Abe et al. observed laser-induced fluorescence (LIF) and dispersed fluorescence (DF) spectra of the jet-cooled 1:1 clusters of phenol with ethanol and many other proton-accepting molecules.[5,6] Because of the high band density near the phenol−EtOH origin, they proposed that the first two transitions, separated by 15 cm^{-1}, should belong to two rotational isomers. Later on, Lipert and Colson disproved this assumption using UV−UV spectral hole-burning (SHB).[27] They probed the intense S_1 state origin and found all transitions of the resonant two-photon ionization (R2PI) spectrum in the SHB spectrum. Hartland et al. used ionization-loss stimulated Raman spectroscopy (ILSRS) to measure frequency shifts of S_0 state vibrations of phenol−EtOH.[28] Cordes et al. studied the complex by two-color R2PI and zero kinetic energy (ZEKE) photoelectron spectroscopy. They measured the inter- and intramolecular vibrations in a range of more than 1700 cm^{-1} and determined the ionization energy of this cluster to be 62901 $\pm$ 5 cm^{-1}.[29] Neither of the two groups could identify a second isomer of the phenol−EtOH cluster.

In contrast to these investigations, we show the existence of at least two conformers of phenol−EtOH in a molecular beam

---

* To whom correspondence should be addressed.

[†] Present address: School of Chemistry, University of Leeds, Leeds, LS2 9JT, UK.

10.1021/jp9907490 CCC: $18.00

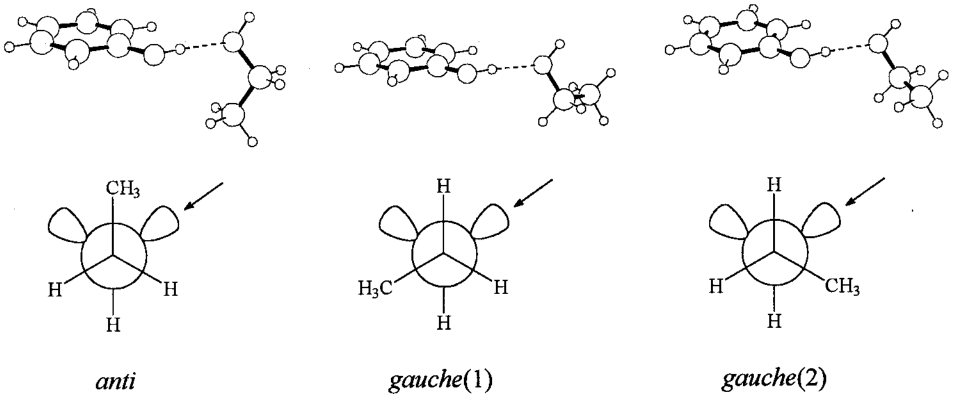

Figure 1. Calculated minimum energy structures of phenol−(EtOH)$_1$. The anti/gauche nomenclature corresponds to the OH torsional conformers of the ethanol moiety. The corresponding Newman projections of ethanol are shown below. The position of phenol is indicated by arrows.

by means of DF spectroscopy and IR−UV and UV−IR double-resonance techniques, complemented and supported by ab initio calculations.

2. Experimental Section

The experimental setup has been described previously.[7] Briefly, ethanol was cooled to −5 °C and its vapor carried with helium (2−3 bar) over phenol at room temperature. The gas mixture coexpanded through a 500 μm pulsed nozzle (see ref 7 for details of the LIF and DF spectroscopy).

IR−UV hole-burning spectroscopy is a double-resonance technique, where a frequency-tuned IR burn laser fires a short time (40−50 ns) before the frequency-fixed UV analysis laser fires.[35,38] If the IR frequency matches a vibrational resonance sharing a common ground-state level with the UV transition analyzed by R2PI, one can observe a decrease of the R2PI signal.

By analogy, in UV−IR SHB spectroscopy the IR laser is frequency-fixed at a selected vibrational transition, while the frequency of the UV analysis laser is scanned. Again, transitions with a common ground state can be detected by a decrease of the R2PI signal. This technique is an alternative to UV−UV SHB if IR transitions belonging to different ground-state levels are well separated and the UV transitions are not.

Phenol (Riedel de Haën) and ethanol (Merck) were of analytical or spectroscopic grade and used without further purification.

3. Theoretical Results

The minimum energy structures of possible phenol−EtOH conformers were calculated at the HF level with the 6-31G(d,p) basis set by using the Gaussian 94 program package.[30] The SCF convergence criterion was 10^{-8} hartree; the convergence criteria for the structural gradient optimization were 1.5×10^{-5} hartree/bohr and 1.5×10^{-5} hartree/deg, respectively. The vibrational frequencies were obtained by performing a normal-mode analysis on the optimized geometries using analytical gradients of the energy.

The HF energy difference between the cluster and the separated monomers is taken as the stabilization energy of the cluster. To calculate its basis set superposition error, the counterpoise method of Boys and Bernardi[31] has been used. The resulting energy difference is D_e. D_0 also includes the zero-point vibrational energy (ZPE).

TABLE 1: Binding Energies in cm^{-1} of the Phenol−EtOH Conformers Shown in Figure 1, Calculated at the HF/6-31G(d,p) Level[a]

HF energy	anti	gauche(1)	gauche(2)
SCF stabiliziation energy	−2620	−2578	−2642
D_e	−2030	−2112	−2152
D_0	−1569	−1696	−1687

[a] D_e: after counterpoise correction. D_0: after zero-point energy and counterpoise correction (see text).

TABLE 2: Calculated Harmonic Frequencies in cm^{-1} and Approximate Description (See Text) of the Vibrations from Normal-Mode Analysis at the HF/6-31G(d,p) Level of the Phenol−EtOH Conformers, Shown in Figure 1[a]

anti		gauche(1)		gauche(2)	
20	ρ_2	14	ρ_2	14	ρ_2
33	τ	21	β_2	32	β_2
37	β_2	27	τ	38	τ
72	ρ_1	67	β_1	66	β_1
77	β_1	77	ρ_1	89	ρ_1
150	σ	136	σ	161	σ
2889	$\nu_{sy}(CH_2)$	2893	$\nu_{sy}(CH_3)$	2892	$\nu_{sy}(CH_3)$
2907	$\nu_{sy}(CH_3)$	2904	$\nu_{sy}(CH_2)$	2905	$\nu_{sy}(CH_2)$
2920	$\nu_{as}(CH_2)$	2949	$\nu_{as}(CH_3)$	2949	$\nu_{as}(CH_3)$
2972	$\nu_{as}(CH_3)$	2972	$\nu_{as}(CH_2+CH_3)$	2974	$\nu_{as}(CH_2+CH_3)$
2983	$\nu_{as}(CH_3)$	2982	$\nu_{as}(CH_2+CH_3)$	2983	$\nu_{as}(CH_2+CH_3)$
3034	CH(Ph)	3034	CH(Ph)	3034	CH(Ph)
3042	CH(Ph)	3042	CH(Ph)	3043	CH(Ph)
3055	CH(Ph)	3055	CH(Ph)	3054	CH(Ph)
3064	CH(Ph)	3064	CH(Ph)	3064	CH(Ph)
3071	CH(Ph)	3071	CH(Ph)	3071	CH(Ph)
3512	OH(Ph)	3513	OH(Ph)	3508	OH(Ph)
3666	OH(EtOH)	3660	OH(EtOH)	3659	OH(EtOH)

[a] In the upper part the intermolecular vibrations are given. The corresponding normal-mode motions are visualized in ref 37. For the nomenclature see refs 32 and 36. The scaled intramolecular CH and OH stretching vibrations are listed in the lower part of the table. For scaling factors see text.

We found three comparably stable isomers of phenol−EtOH, which correspond to the anti and both gauche rotamers of ethanol (Figure 1 and Table 1). Note that in contrast to the monomer, the gauche(1) and gauche(2) structures have slightly different energies because of their nonequivalent interaction with the phenol moiety. Structures with ethanol acting as proton acceptor turn out to be the most stable ones. This acceptor interaction should induce a red shift of the S_0−S_1 excitation energy compared to that of bare phenol.[1] We did not find any minimum energy structures, where the ethanolic H−O−C plane is parallel to the aromatic π-system.

Table 1 shows the stabilization energies of all three clusters. These energies differ only by 10−130 cm^{-1}, so on this level of theory it is not possible to decide which structure is the most stable one. The calculated binding energies range from 1569 to 1696 cm^{-1} and are comparable to a binding energy of 1551

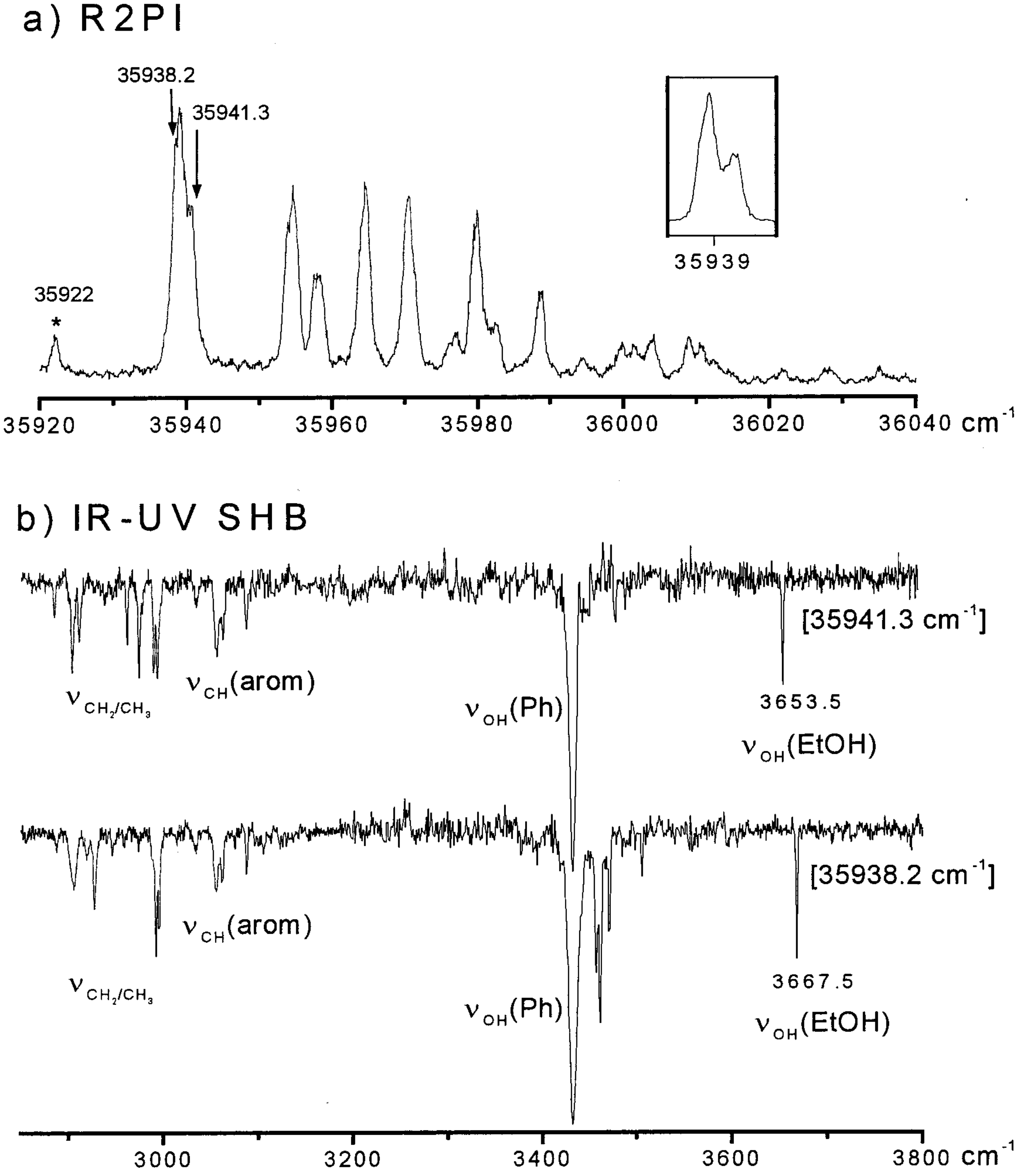

Figure 2. (a) One-color R2PI spectrum of phenol−(EtOH)$_1$. The inset shows the S$_1$ state origin at better resolution with two transitions clearly distinguishable. The spectral positions for IR−UV SHB analysis are marked by arrows. The small band at 35 922 cm^{-1} is a hot band. (b) IR−UV SHB of both S$_1$ state origin transitions, analyzed at the red and blue wing (lower and upper traces, respectively). While the phenolic CH and phenolic OH stretching vibrations are quite similar, the corresponding ethanolic vibrations show considerable differences. The four transitions between 3455 and 3505 cm^{-1} can only be observed in the spectrum analyzed at 35 938.2 cm^{-1} because of the larger analysis signal here. These bands can be interpreted as combination bands (see text).

cm^{-1} for the phenol−(H$_2$O)$_1$ cluster at the same level of theory.[32]

The calculated intermolecular vibrations and intramolecular CH and OH stretching frequencies are listed in Table 2. The CH stretching vibrations are scaled by a factor of 0.91 obtained from ref 33. The scaling factors for the phenolic ($f = 0.865$) and ethanolic ($f = 0.876$) OH stretching modes are obtained from the comparison of experimental and theoretical data of the phenol−(H$_2$O)$_1$ cluster and bare ethanol, respectively.

For all three calculated structures, the phenolic OH stretching frequencies are nearly equal. The two gauche clusters show very similar intramolecular vibrations, which differ significantly from those of the anti conformer. According to earlier investigations of bare ethanol,[26] the OH stretching vibration of the anti conformer is blue-shifted (about 7 cm^{-1}) relative to that of the gauche structure. There are also some notable differences in the frequency pattern of the aliphatic CH stretching vibrations between anti and gauche. Krueger et al. explained the OH and CH frequency shifts by the participation of the lone pair at the ethanolic oxygen atom in the adjacent σ^* CH orbital in the trans position. This interaction should raise ν(OH) as the s-character of that bond increases and lower ν(CH) due to the decreasing s-character.[22] In the gauche conformer there is one and in the anti conformer there are two of those trans lone pair interactions (Figure 1). Inspection of the IR spectra of several primary, secondary, and tertiary alcohols showed that the frequency shift of the OH and CH stretching vibrations is proportional to the number of trans interactions.[18,22] Thus, we expect that $\nu(\mathrm{OH})_{\mathrm{anti}}$

$> \nu(\mathrm{OH})_{\mathrm{gauche}}$ and $\nu(\mathrm{CH_2})_{\mathrm{anti}} < \nu(\mathrm{CH_2})_{\mathrm{gauche}}$. Our calculations indeed show these shifts (Table 2).

The low-energy intermolecular vibrations differ significantly for the three calculated conformers (Table 2). It has been shown for several phenol clusters[7,32,33] that the experimental and calculated HF/6-31G** intermolecular frequencies can be compared without scaling.

4. Experimental Results and Discussion

Figure 2a shows the one-color R2PI spectrum of phenol−(EtOH)$_1$ on the 140 amu mass trace from 35 920 to 36 040 cm^{-1}. We recorded simultaneously the higher clusters (n = 2−5) to exclude the possibility that bands presented in Figure 2a are because of fragmentation onto the n = 1 mass trace. The electronic origin consists of two transitions with maxima at 35 938.7 and 35 940.3 cm^{-1} and an intensity ratio of (2−3):1. The intensity ratio of these two bands remained unchanged at higher stagnation pressures of helium, while the band at 35 922 cm^{-1} disappeared (hot band). The hitherto unobserved[5,27,29] transition at 35 940.3 cm^{-1} nearly completely disappeared when the helium seed gas was substituted by a rare gas mixture of helium and neon (70:30). All other vibronic transitions in Figure 2a are well-known from previous investigations.[5,27,29]

The IR−UV SHB spectra of the two transitions analyzed at 35 941.3 and 35 938.2 cm^{-1} are shown in Figure 2b. The band observed in both spectra at 3432 cm^{-1} is assigned to the phenolic OH stretching vibration and fits the corresponding calculated (and scaled) transitions reasonably well (Table 2). Like the phenol−(H$_2$O)$_1$ complex, this band is strongly red-shifted relative to that of bare phenol (3531 relative to 3657 cm^{-1} [34]), because of a strong hydrogen bond, which weakens the phenolic OH bond. We noticed that the width of the rather broad phenolic OH stretching bands sensitively depends on the IR laser intensity. By lowering the IR energy from 2.5 to 0.5 mJ/pulse (IR beam diameter of 1−2 mm, pulse width of <10 ns), we observed a line width decrease from 15.6 to 6.5 cm^{-1} (Figure 3). Obviously, there is considerable laser power broadening at these IR intensities, which are typical for many IR−UV experiments in the literature.[8,9,34,35,38] This power broadening has to be investigated before dynamical reasons are considered to explain IR−UV bandwidths.

Even at the lowest laser energies we could not detect any frequency difference between the phenolic OH stretching vibration in the two spectra. The aromatic CH stretching frequencies of the phenol moiety in the range 3020−3100 cm^{-1} are also nearly identical in both spectra (Table 3).

The remaining transitions can be attributed to the ethanolic moiety of the cluster. The bands at 3653 and 3667 cm^{-1} can be assigned easily to the ethanolic OH stretching vibration. The large frequency difference points to two different ethanol conformers. The observed OH frequencies correspond well to the different OH stretching frequencies of the gauche and anti isomers of bare ethanol in the gas phase (3660 and 3676 cm^{-1} [16]) or trapped in argon matrixes (3656 and 3661 cm^{-1} [21]). Note that the calculated ethanolic OH stretching vibrations also reflect the gauche/anti frequency shift (Table 2). Thus, we tentatively assign the IR spectrum analyzed at 35 941.3 cm^{-1} to the gauche conformer and the spectrum analyzed at 35 938.2 cm^{-1} to the anti conformer.

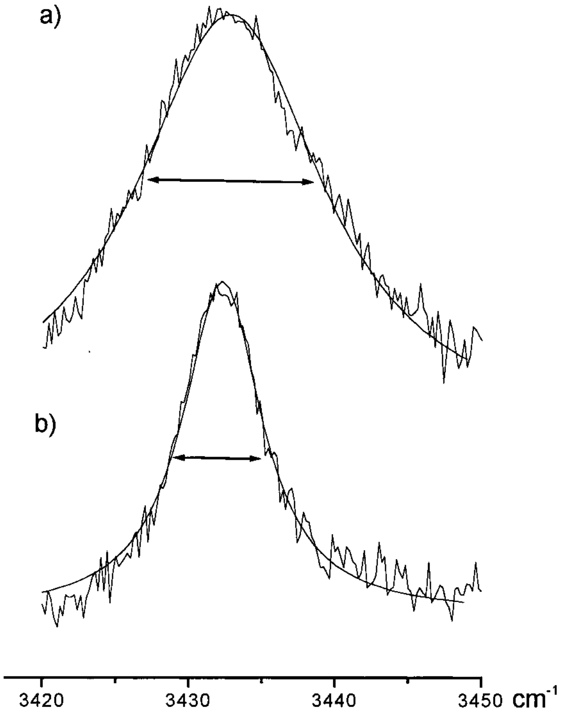

Figure 3. IR−UV SHB spectra of the phenolic OH stretching mode of phenol−EtOH analyzed at 35 941.3 cm^{-1} and measured with different IR power. The full bandwidth at half-maximum (fwhm) clearly depends on the IR intensity used: (a) fwhm = 15.6 cm^{-1}, power = 2.5 mJ/pulse; (b) fwhm = 6.5 cm^{-1}, power = 0.5 mJ/pulse.

TABLE 3: Comparison of the Experimental Vibrational Frequencies of the Ground State of Phenol−EtOH and the Calculated Harmonic Frequencies of the Anti- and Gauche(2) Rotamers[a]

anti			gauche(2)		
exptl	calcd	assignt	exptl	calcd	assignt
22	20	ρ_2	19	14	ρ_2
25	33	τ	33	32	β_2
45	37	β_2	43	38	τ
67/71	72	ρ_1	65	−| 66	$2\beta_2 \| \beta_1$
77	77	β_1	75	89	ρ_1
89		$2\beta_2$	96		$3\beta_2 \| \beta_2 + \beta_1$
153	150	σ	162	161	σ
174		$\sigma + \rho_2$	194		$\sigma + \beta_2$
177		$\sigma + \tau$			
2888		b	2885		b
2905	2889	$\nu_{sy}(\mathrm{CH_2})$	2903	2892	$\nu_{sy}(\mathrm{CH_3})$
2919	2907	$\nu_{sy}(\mathrm{CH_3})$	2911	2905	$\nu_{sy}(\mathrm{CH_2})$
2927	2920	$\nu_{as}(\mathrm{CH_2})$	2961	2949	$\nu_{as}(\mathrm{CH_2/CH_3})^d$
2992	2972	$\nu_{as}(\mathrm{CH_3})$	2974		c
2995	2983	$\nu_{as}(\mathrm{CH_3})$	2989	2974	$\nu_{as}(\mathrm{CH_2/CH_3})^d$
3035	3034	CH(Ph)	2993	2983	$\nu_{as}(\mathrm{CH_2/CH_3})^d$
	3042	CH(Ph)	3033	3034	CH(Ph)
3055	3055	CH(Ph)		3043	CH(Ph)
3061	3064	CH(Ph)	3056	3054	CH(Ph)
3087	3071	CH(Ph)	3062	3064	CH(Ph)
3432	3512	OH(Ph)	3087	3071	CH(Ph)
3667	3666	OH(EtOH)	3432	3508	OH(Ph)
			3653	3659	OH(EtOH)

[a] The calculated intramolecular CH and OH stretching vibrations in the lower part are scaled (see text). The vertical slashs indicate alternative assignments. [b] Overtone or combination band. [c] Combination band. [d] With contributions from the antisymmetric CH$_2$ and CH$_3$ stretching vibration.

The ethanolic CH vibrations are observed in the frequency range 2880−3000 cm^{-1} (Figure 2 and Table 3). All three CH$_3$ vibrations and the two CH$_2$ vibrations are observed in both spectra. The vibrational pattern differs considerably. The most remarkable effect is the red shift of the CH$_2$ vibrations in the spectrum analyzed at 35 938.2 cm^{-1}. A red shift of the CH$_2$ vibrational frequencies is expected from the stronger trans lone pair effect in the anti conformer. Hence, both the blue shift of the OH vibrations and the red shift of the CH$_2$ vibrations support

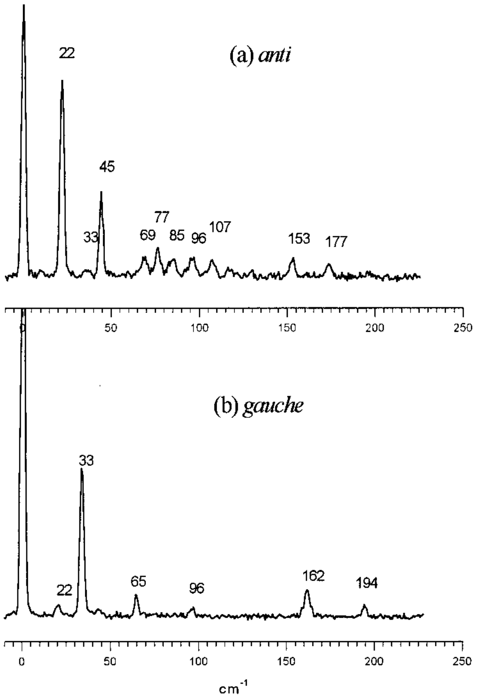

Figure 4. DF spectra of the electronic origin of phenol−(EtOH)$_1$ analyzed at (a) 35 938.2 cm^{-1} and (b) 35 941.3 cm^{-1}. Note the very different vibrational pattern in the two spectra.

our assignment of the transitions with maxima at 35 938.7 and 35 940.3 cm^{-1} as electronic origins of the phenol clusters with the anti and gauche conformers of ethanol, respectively.

By a simple comparison of the UV intensities, it seems that in contrast to our calculations the anti conformer is more stable than the gauche conformer. The calculations point to very similar stabilization energies of the two gauche isomers. The second gauche isomer was not detectable either because of the small concentration in the molecular beam or because of accidental overlapping of band systems.

For a comparison of the low-energy vibrations of the two conformers in the electronic ground state, DF spectra were recorded by excitation of different vibronic transitions (see Figures 4 and 5). The remarkable differences between the DF spectra of the two origin bands strengthen the hypothesis that they belong to different species. The transitions at 22, 45, 153, and 177 cm^{-1} are characteristic for the isomer analyzed at 35 938.2 cm^{-1}, while the transitions at 33, 162, and 194 cm^{-1} are characteristic for the other isomer (Figure 4). The small bands at 22 cm^{-1} in Figure 4b and 33 cm^{-1} in Figure 4a can be explained by simultaneous excitation of the respective other isomer because of overlapping origin bands. We assign the bands at 153 and 162 cm^{-1} to the intermolecular stretching vibrations of the two isomers, which are clearly separated from the low-energy torsion and bending vibrations. A comparison with the calculated S_0 state vibrations in Table 3 shows that the σ-vibrations of the anti and the gauche(2) conformer at 150 and 161 cm^{-1}, respectively, fit surprisingly well. This is also in accord with the anti/gauche assignment from IR−UV SHB spectroscopy. The intermolecular stretch of the gauche(1) conformer is calculated to be at 136 cm^{-1} but is not observed. The σ-vibration in the S_1 state has been observed at 162 cm^{-1} [29] and probably belongs to the anti conformer.

For better isomer assignment, we analyzed the R2PI spectra after pumping the well-separated 3653 and the 3667 cm^{-1} IR transitions of the two isomers. This seemed to be more promising than using UV−UV double-resonance spectroscopy because of the strongly overlapping vibronic spectra. The resulting UV−IR spectra and the difference spectrum are displayed in Figure 5. Figure 5b shows that the transitions at 35 940 + 31 and +42 cm^{-1} belong mainly to the higher energy component of the electronic origin (gauche isomer), while the other transitions and the hot band at 35 922 cm^{-1} nearly exclusively belong to the anti conformer. Interestingly, the rather intense and comparatively well-separated intermolecular gauche band at 31 cm^{-1} also appears in the UV−UV SHB spectrum of Lipert and Colson.[27]

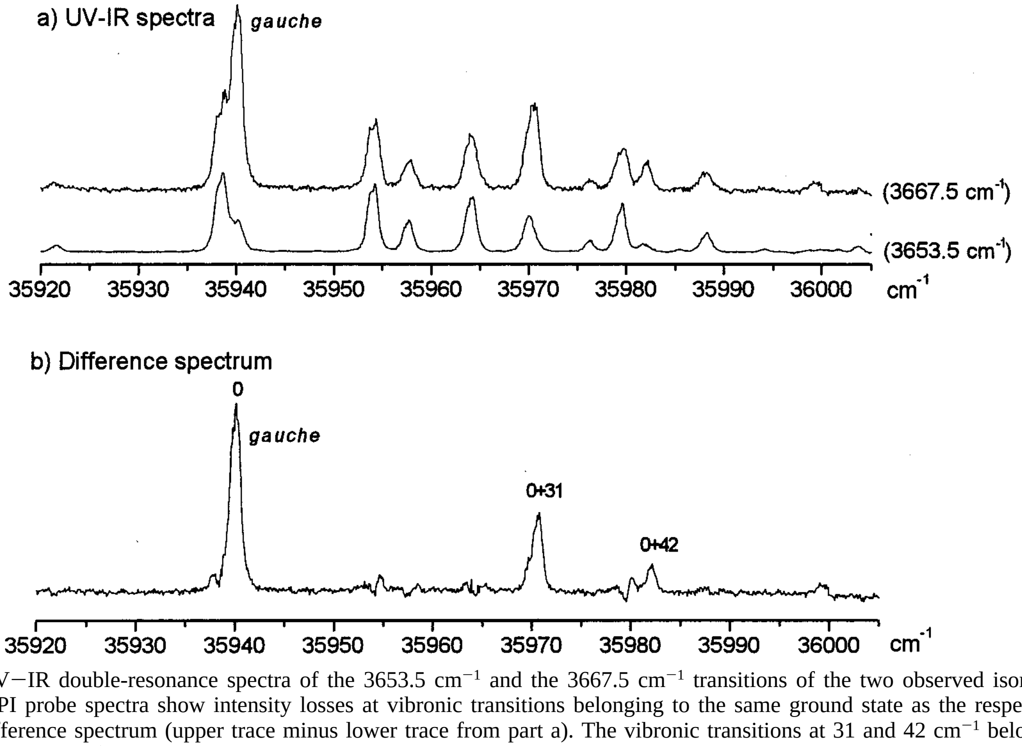

Figure 5. (a) UV−IR double-resonance spectra of the 3653.5 cm^{-1} and the 3667.5 cm^{-1} transitions of the two observed isomers of phenol−(EtOH)$_1$. The R2PI probe spectra show intensity losses at vibronic transitions belonging to the same ground state as the respective pumped IR transition. (b) Difference spectrum (upper trace minus lower trace from part a). The vibronic transitions at 31 and 42 cm^{-1} belong to the isomer with origin at 35 940.2 cm^{-1} (gauche isomer).

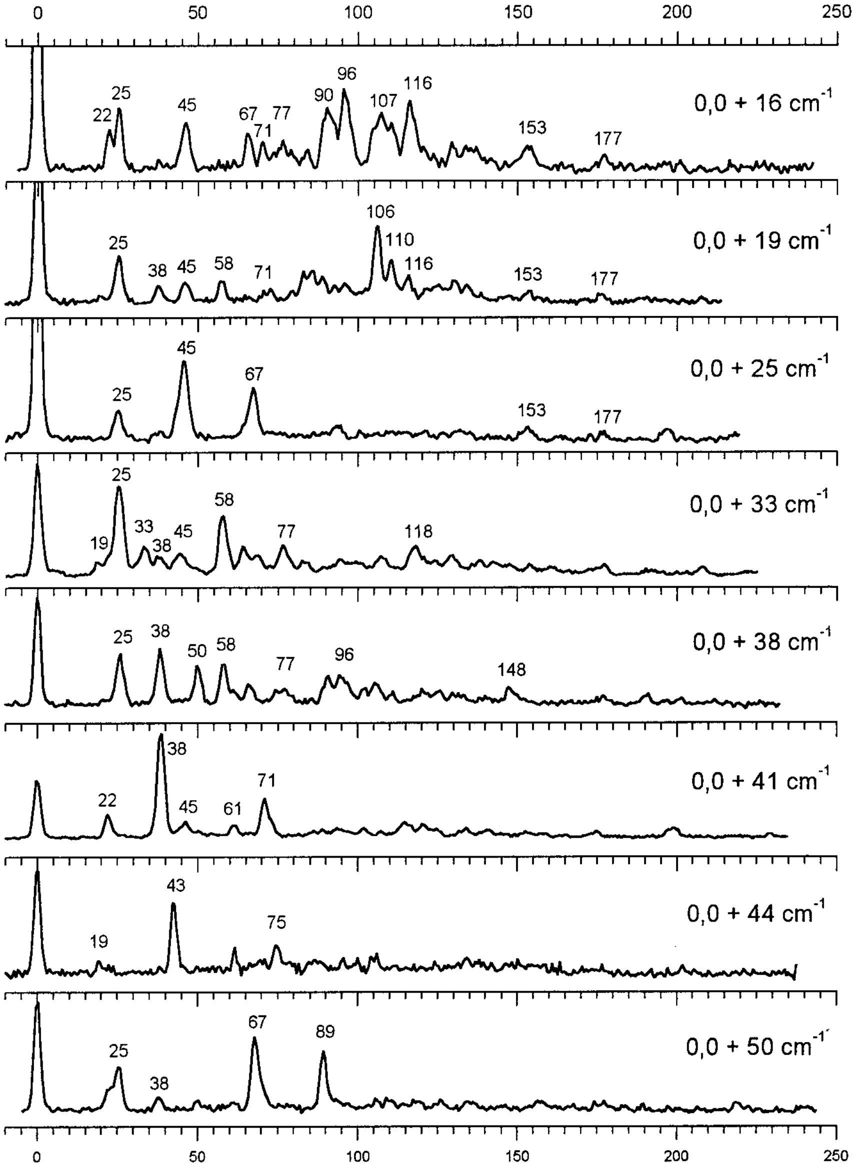

Figure 6. DF spectra of the first eight vibronic transitions of the phenol−(EtOH)$_1$ complex. The vibronic S$_1$-state transitions at +33 and +44 cm^{-1} relative to the 35 938 cm^{-1} origin belong mainly to the isomer with origin at 35 940 cm^{-1}. The bands at 35938 + 33/+44 cm^{-1} correspond to 35 940 + 31/+42 cm^{-1} (Figure 5).

The DF spectra of the eight most intense low-frequency vibronic transitions are presented in Figure 6. The analyzed transitions at 35 938 + 16/+19/+25 cm^{-1} correlate to the S$_0$ vibrations at +22/+25/+45 cm^{-1} according to the propensity rule. They can be assigned to the calculated anti conformer vibrational modes of lowest energy ρ_2, τ, and β_2 (Tables 3 and 4). In contrast to our assignment, the group of Abe et al. correlated $+25(S_1) \leftrightarrow +22(S_0)$.[6]

As shown above, the transitions at 35 938 + 33/+44 cm^{-1} mainly belong to the gauche conformer. The corresponding DF spectra show ground-state vibrations at 19 and 43 cm^{-1}, which are not observed in the other DF spectra and can therefore be assigned to S$_0$ gauche vibrations. Further transitions in the DF spectra can be explained as combination bands and overtones of the fundamental modes, and the most obvious assignments are given in Table 3. Note that the intense S$_0$ vibration at 38 cm^{-1} evidently correlates to the S$_1$ vibration at 41 cm^{-1} but could not be explained by any of the calculated vibrational modes.

The DF spectra may help to further interpret the S$_0$ state IR spectra. The lower trace of Figure 2b shows four transitions with a blue shift of 25, 29, 39, and 73 cm^{-1} relative to the phenolic OH stretching vibration of the anti isomer, which are only detectable at very high IR intensities of about 2−3 mJ/

TABLE 4: Assignment of the Low-Energy S$_1$-State Transitions to the Phenol−EtOH Conformers Anti and Gauche(2)

exptl S$_1$ transition (rel to 35 938 cm^{-1})	assignment	
	anti	gauche(2)
16	ρ_2	
19	τ	
25	β_2	
33	$(2\,\rho_2)$	β_2
38	$2\,\tau$	
41	$\|\rho_2 + \beta_2{}^{c}$	
44	$(\tau + \beta_2)$	τ
50	$2\beta_2$	
162[b]	σ	

[a] The fundamental vibrations are correlated to the corresponding ground-state vibrations (see Table 3). The parentheses indicate probable small contributions from the anti conformer to the gauche spectrum. The vertical slash indicates alternative assignments. [b] Reference 29. [c] Correlates with the unknown S$_0$ 38 cm^{-1} transition.

pulse. They can be interpreted as combination bands of the phenolic OH vibration with the intermolecular modes at 22, 25, 38, and 71(77) cm^{-1}.

5. Summary and Conclusions

The phenol−(ethanol)$_1$ cluster was studied by means of R2PI, IR−UV, and UV−IR double-resonance and DF spectroscopy. Combining the experimental results with theoretical results from ab initio calculations, we can assign the observed bands as arising from an anti and a gauche conformer of the ethanol moiety. This is in contrast to earlier publications, which concluded from their measurements[27,29] the existence of only one isomer. The small frequency shift of the electronic origins of less than 2 cm^{-1} may explain why they were not discriminated before. A further reason might be the dependence of the rotamer population from the seed gas composition. Although in He the anti/gauche ratio was (2−3):1, it was at least 50:1 in a He:Ne (70:30) mixture. The R2PI spectrum in ref 29 was measured with an argon-seeded molecular beam, and the observed spectral bandwidths were somewhat larger than in our spectra. This effect or a preference for the anti conformer in the argon beam may explain the lack of resolved gauche signals in ref 29.

Acknowledgment. This paper is part of the doctoral thesis of P.I., C.J., and D.S. The authors thank the Universitätsrechenzentrum Düsseldorf for the granted computing time and the Deutsche Forschungsgemeinschaft (DFG) and the Fond der chemischen Industrie for financial support.

References and Notes

(1) Pohl, M.; Schmitt, M.; Kleinermanns, K. *J. Chem. Phys.* **1991**, *94*, 1717.

(2) Yi, M.; Scheiner, S. *Chem. Phys. Lett.* **1996**, *262*, 567.

(3) Schiefke, A.; Deusen, C.; Jacoby, Ch.; Gerhards, M.; Schmitt, M.; Kleinermanns, K. *J. Chem. Phys.* **1995**, *102*, 9197.

(4) Iwasaki, A.; Fujii, A.; Watanabe, T.; Ebata, T.; Mikami, N. *J. Phys. Chem.* **1996**, *100*, 16053.

(5) Abe, H.; Mikami, N.; Ito, M. *J. Phys. Chem.* **1982**, *86*, 1768.

(6) Abe, H.; Mikami, N.; Ito, M. *J. Phys. Chem.* **1982**, *86*, 2567.

(7) Jacoby, Ch.; Roth, W.; Schmitt, M.; Janzen, Ch.; Spangenberg, D.; Kleinermanns, K. *J. Phys. Chem. A* **1998**, *102*, 4471.

(8) Imhof, P.; Roth, W.; Janzen, Ch.; Spangenberg, D.; Kleinermanns, K. *Chem. Phys.* **1999**, *242*, 141−151, 153−159.

(9) Pribble, R. N.; Zwier, T. S. *Science* **1994**, *265*, 74.

(10) Buck, U.; Ettischer, I.; Melzer, M.; Buch, V.; Sadlej, J. *Phys. Rev. Lett.* **1998**, *80*, 2578.

(11) Roth, W.; Schmitt, M.; Jacoby, Ch.; Spangenberg, D.; Janzen, Ch.; Kleinermanns, K. *Chem. Phys.* **1998**, *239*, 1. Janzen, Ch.; Spangenberg, D.; Roth, W.; Kleinermanns, K. *J. Chem. Phys.* **1999**, *110*, 9898.

(12) Badger, R. M.; Bauer, S. H. *J. Chem. Phys.* **1936**, *4*, 711.

(13) Perchard, J.-P.; Josien, M.-L. *J. Chim. Phys. Phys.−Chim. Biol.* **1968**, *65*, 1834.

(14) Durig, J. R.; Bucy, W. E.; Wurrey, C. J.; Carreira, L. A. *J. Phys. Chem.* **1975**, *79*, 988.

(15) Richter, W.; Schiel, D. *Ber. Bunsen-Ges. Phys. Chem.* **1981**, *85*, 548.

(16) Fang, H. L.; Swofford, R. L. *Chem. Phys. Lett.* **1983**, *105*, 5.

(17) Ehrbrecht, M.; Huisken, F. *J. Phys. Chem. A* **1997**, *101*, 7768.

(18) Oki, M.; Iwamura, H. *Bull. Chem. Soc. Jpn.* **1959**, *32*, 950.

(19) Belhekar, A. A.; Agashe, M. S.; Jose, C. I. *J. Chem. Soc., Faraday Trans.* **1990**, *86*, 1781.

(20) Barnes, A. J.; Hallam, H. E. *Trans. Faraday Soc.* **1970**, *66*, 1932.

(21) Coussan, S.; Bouteiller, Y.; Perchard, J. P.; Zheng, W. Q. *J. Phys. Chem. A* **1998**, *102*, 5789.

(22) Krueger, P. J.; Jan, J.; Wieser, H. *J. Mol. Struct.* **1970**, *5*, 375.

(23) Kakar, R. K.; Quade, C. R. *J. Chem. Phys.* **1980**, *72*, 4300.

(24) Dothe, H.; Lowe, M. A.; Alper, J. S. *J. Phys. Chem.* **1989**, *93*, 6632.

(25) Shaw, R. A.; Wieser, H.; Dutler, R.; Rauk, A. *J. Am. Chem. Soc.* **1990**, *112*, 5401.

(26) Bakke, J. M.; Bjerkeseth, L. H. *J. Mol. Struct.* **1997**, *407*, 27.

(27) Lipert, R. J.; Colson, S. D. *J. Phys. Chem.* **1989**, *93*, 3894.

(28) Hartland, G. V.; Henson, B. F.; Venturo, V. A.; Felker, P. M. *J. Phys. Chem.* **1992**, *96*, 1164.

(29) Cordes, E.; Dopfer, O.; Wright, T. G.; Müller-Dethlefs, K. *J. Phys. Chem.* **1993**, *97*, 7471.

(30) Frisch, M. J.; Trucks, G. W.; Schlegel, H. B.; Gill, P. M. W.; Johnson, B. G.; Robb, M. A.; Cheeseman, J. R.; Keith, T.; Petersson, G. A.; Montgomery, J. A.; Raghavachari, K.; Al-Laham, M. A.; Zakrzewski, V. G.; Ortiz, J. V.; Foresman, J. B.; Cioslowski, J.; Stefanov, B. B.; Nanayakkara, A.; Challacombe, M.; Peng, C. Y.; Ayala, P. Y.; Chen, W.; Wong, M. W.; Andres, J. L.; Replogle, E. S.; Gomperts, R.; Martin, R. L.; Fox, D. J.; Binkley, J. S.; Defrees, D. J.; Baker, J.; Stewart, J. P.; Head-Gordon, M.; Gonzalez, C.; Pople, J. A. *Gaussian 94*, revision E.2; Gaussian, Inc.: Pittsburgh, PA, 1995.

(31) Boys, S. F.; Bernardi, F. *Mol Phys.* **1970**, *19*, 553.

(32) Schütz, M.; Bürgi, Th.; Leutwyler, S. *J. Chem. Phys.* **1993**, *98*, 3763.

(33) Schütz, M.; Bürgi, Th.; Leutwyler, S.; Fischer, T. *J. Chem. Phys.* **1995**, *103*, 6350.

(34) Watanabe, T.; Ebata, T.; Tanabe, S.; Mikami, N. *J. Chem. Phys.* **1996**, *105*, 408.

(35) Brutschy, B. *Chem. Rev.* **1992**, *92*, 1567.

(36) Gerhards, M.; Beckmann, K.; Kleinermanns, K. *Z. Phys.* D **1994**, *29*, 223.

(37) http://www-public.rz.uni-duesseldorf.de/∼pc1/abinitio/.

(38) Gerhards, M.; Schiwek, M.; Unterberg, C.; Kleinermanns, K. *Chem. Phys. Lett.* **1998**, *297*, 515.